Numerical Computation of the Linear Stability of the Diffusion Model for Crystal Growth Simulation

Daniel Meiron
Daniel Sorensen
Elizabeth Wedeman
Chao Yang

CRPC-TR96645-S
March 1996

Center for Research on Parallel Computation
Rice University
6100 South Main Street
CRPC - MS 41
Houston, TX 77005

NUMERICAL COMPUTATION OF THE LINEAR STABILITY OF THE DIFFUSION MODEL FOR CRYSTAL GROWTH SIMULATION

C. YANG *, D. C. SORENSEN †, D. I. MEIRON ‡ AND B. WEDEMAN §

Abstract. We consider a computational scheme for determining the linear stability of a diffusion model arising from the simulation of crystal growth. The process of a needle crystal solidifying into some undercooled liquid can be described by the dual diffusion equations

$$\frac{\partial U_l}{\partial t} = \alpha \nabla^2 U_l, \quad \frac{\partial U_s}{\partial t} = \alpha \nabla^2 U_s,$$

with appropriate initial and boundary conditions. Here U_l and U_s denote the temperature of the liquid and solid respectively, and α represents the thermal diffusivity. At the solid-liquid interface, the motion of the interface denoted by $\vec{r}$ and the temperature field are related by the conservation relation

$$\frac{d\vec{r}}{dt} \cdot \vec{n} = \alpha(\nabla U_s \cdot \vec{n} - \nabla U_l \cdot \vec{n}),$$

where $\vec{n}$ is the unit outward pointing normal to the interface. A basic stationary solution to this free boundary problem can be obtained by writing the equations of motion in a moving frame and transforming the problem to parabolic coordinate system. This is known as the Ivantsov parabola solution. Linear stability theory applied to this stationary solution gives rise to an eigenvalue problem of the form

$$\begin{aligned} \frac{1}{\eta^2+\xi^2}\left[\frac{\partial^2 U}{\partial \xi^2} + \frac{\partial^2 U}{\partial \eta^2} + 2P\left(\eta\frac{\partial U}{\partial \eta} - \xi\frac{\partial U}{\partial \xi}\right)\right] &= \lambda U, \\ \frac{-1}{1+\xi^2}\left[\frac{\partial U}{\partial \eta} + 4P^2 N + 2P(N + \xi\frac{\partial N}{\partial \xi})\right] &= \lambda N, \\ U = 2PN \quad \text{at } \eta = 1. \end{aligned}$$

The largest real part of the eigenvalue λ is proportional to the growth rate of the perturbation, and the eigenfunction is related to the perturbation of the temperature field and the interface geometry. Numerical solution of the above equations is based on a finite difference discretization. The corresponding large scale algebraic eigenvalue problem is solved by ARPACK, a software package that implements the Implicitly Restarted Arnoldi Method (IRAM.)

Accurate computation of these eigenvalues helps to determine interesting unstable modes that involve excitation of the interface. Analysis suggests that at least part of the spectrum corresponding to this eigenvalue problem is continuous and unbounded. In addition computation via standard methods such as QR becomes expensive when the mesh size of the discretization becomes small. We find however that IRAM is very efficient in extracting eigenvalues and eigenvectors of interest with modest cost. Numerical results will be presented to demonstrate the effectiveness this method.

* Department of Computational and Applied Mathematics, Rice University, Houston, Texas 77251, USA; E-Mail: chao@caam.rice.edu .

† Department of Computational and Applied Mathematics, Rice University, Houston, Texas 77251, USA; E-Mail: sorensen@caam.rice.edu.

‡ Department of Applied Mathematics, California Institute of Technology, Pasadena, California 91125, USA; E-Mail: dim@ama.caltech.edu.

§ Department of Applied Mathematics, California Institute of Technology, Pasadena, California 91125, USA; E-Mail: bw@ama.caltech.edu.

1. Introduction. There has been a great deal of interest in the simulation and modeling of crystal growth and dentridic solidification in the past few years [2] [6]. It is well known that the physical behavior of a needle crystal solidifying into some undercooled liquid can be described by the dual diffusion equations

$$\frac{\partial U_l}{\partial t} = \alpha \nabla^2 U_l, \quad \frac{\partial U_s}{\partial t} = \alpha \nabla^2 U_s, \tag{1}$$

Here U_l and U_s denote the temperature of the liquid and solid respectively. They are functions of the time t and the spatial coordinates x and z. The parameter α represents the thermal diffusivity. At the solid-liquid interface, $U_l = U_s$, and the motion of the interface denoted by $\vec{r}$ and the temperature field are related by the conservation relation

$$\frac{d\vec{r}}{dt} \cdot \vec{n} = \alpha(\nabla U_s \cdot \vec{n} - \nabla U_l \cdot \vec{n}), \tag{2}$$

where $\vec{n}$ is the unit outward pointing normal to the interface. It is also natural to impose the boundary condition

$$U_l \to 0, \text{ as } z \to \infty. \tag{3}$$

Both analytical and numerical solutions of (1) and (2) are difficult to obtain because of the moving boundary. We are interested in analyzing the stability of a well known stationary solution that corresponds to a simple parabolic shaped moving front. In the following, we give a brief description of the Ivantsov solution and a standard linear stability analysis that gives rise to an eigenvalue problem. Numerical discretization of the continuous model and the solution of the large scale algebraic eigenvalue problem derived from the discretization are also discussed. It is observed from our numerical computation that the solidification is unstable.

2. Ivantsov solution. A stationary solution of (1) that corresponds to a parabolic shaped moving front can be obtained by the method of Ivantsov [3]. Suppose the front is moving in the z direction with a constant velocity v. We first rewrite the equation (1) in a moving frame. *i.e.*, we let

$$z \leftarrow z - vt \text{ and } x \leftarrow x. \tag{4}$$

After these changes of variables, equations (1) become

$$\nabla^2 U + \frac{2}{l}\frac{\partial U}{\partial z} = \frac{1}{\alpha}\frac{\partial U}{\partial t}, \tag{5}$$

in both the liquid and solid phases. The boundary conditions (2) (3) remain the same. To simplify the geometry, transformations

$$x = \rho\eta\xi \text{ and } z = \rho\frac{\eta^2 - \xi^2}{2} \tag{6}$$

are used to map the parabolic interface in (x, z) coordinate system to the horizontal line $\eta = 1$ in (ξ, η) coordinate system. In these new coordinates, the convection diffusion equation (5) can be written as

$$\frac{\partial^2 U}{\partial \xi^2} + \frac{\partial^2 U}{\partial \eta^2} + 2P\Big(\eta \frac{\partial U}{\partial \eta} - \xi \frac{\partial U}{\partial \xi}\Big) = (\eta^2 + \xi^2) P \frac{\partial U}{\partial \tau}, \tag{7}$$

where $P \equiv \rho/l$ is the *Peclet* number, and τ is defined to be $\tau \equiv (v/2\rho)t$. The boundary condition imposed at the moving front $\eta = 1$ satisfies

$$P\Big[\frac{\partial N}{\partial t}(N^2 + \xi^2) + 2\Big(N + \xi \frac{\partial N}{\partial \xi}\Big)\Big] = \Big(\frac{\partial U_s}{\partial \eta} - \frac{\partial U_l}{\partial \eta}\Big) - \frac{\partial N}{\partial \xi}\Big(\frac{\partial U_s}{\partial \xi} - \frac{\partial U_l}{\partial \xi}\Big). \tag{8}$$

It is easy to verify that a stationary solution to (7) and (8) is in the form

$$\bar{N} = 1, \quad \bar{U}_l = \sqrt{\pi P}\exp(P)\mathrm{erfc}(\sqrt{P}\eta), \text{ and } \bar{U}_s = \sqrt{\pi P}\exp(P)\mathrm{erfc}(\sqrt{P}). \tag{9}$$

3. Linear Stability Analysis. The objective of this paper is to determine the linear stability of the Ivantsov solution under small disturbance. This is done by assuming that there exists a solution to (7) and (8) of the form

$$N = \bar{N} + \tilde{N}\exp(\sigma\tau), \quad U_l = \bar{U}_l + \tilde{U}_l \exp(\sigma\tau), \text{ and } U_s = \bar{U}_s + \tilde{U}_s \exp(\sigma\tau), \tag{10}$$

where $\bar{N}$, $\bar{U}_l$ and $\bar{U}_s$ are stationary solutions derived by Ivantsov method, and σ is the growth rate.

The substitution of (10) into (7) leads to the disturbance equation

$$\Big(\frac{\partial^2 \tilde{U}}{\partial \xi^2} + \frac{\partial^2 \tilde{U}}{\partial \eta^2}\Big) + 2P\Big(\eta \frac{\partial \tilde{U}}{\partial \eta} - \xi \frac{\partial \tilde{U}}{\partial \xi}\Big) = (\eta^2 + \xi^2) P \sigma \bar{U}, \tag{11}$$

in both phases with boundary conditions

$$\begin{aligned} \bar{U}_s = 0 \text{ everywhere}, \quad \bar{U}_l &= -\frac{\partial \tilde{U}_l}{\partial \eta}\tilde{N} \text{ at } \eta = 1 \text{ and} \\ P[\sigma\tilde{N}(1 + \xi^2) + 2(\tilde{N} + \xi\frac{\partial \tilde{N}}{\xi})] &= \Big(-\frac{\partial \tilde{U}_l}{\partial \eta} - 4P^2\tilde{N}\Big), \text{ at } \eta = 1. \end{aligned} \tag{12}$$

To simplify the notation, we rename variables $\tilde{N}$ and $\tilde{U}$ to N and U respectively, and let $\lambda = \sigma P$. Equation (11) and the boundary condition (12) can be written as the following eigenvalue problem:

$$\frac{1}{\eta^2 + \xi^2}\Big[\frac{\partial^2 U}{\partial \xi^2} + \frac{\partial^2 U}{\partial \eta^2} + 2P\Big(\eta \frac{\partial U}{\partial \eta} - \xi \frac{\partial U}{\partial \xi}\Big)\Big] = \lambda U \tag{13}$$

$$-\frac{1}{1 + \xi^2}\Big[\frac{\partial U}{\partial \eta} + 4P^2 N + 2P\Big(N + \xi \frac{\partial N}{\partial \xi}\Big)\Big] = \lambda N \quad (\eta = 1). \tag{14}$$

where U and N are coupled by $U = 2PN$ at $\eta = 1$.

On an infinite domain. The boundary condition at infinity are

$$\frac{\partial U}{\partial \eta} \to 0, \text{ as } \eta \to \pm\infty, \text{ and } \frac{\partial U}{\partial \xi} \to 0, \text{ as } \xi \to \pm\infty.$$

4. Discretization. In our numerical approximation, the infinite domain problem is first transformed into a finite domain problem by using the following change of variables. Let

$$\tilde{s} = \frac{\xi}{1+\xi} \quad \text{and} \quad \tilde{t} = \frac{2\eta}{1+\eta}.$$

In these new variables, (13) and (14) become

$$C(\tilde{s},\tilde{t})\Big[(1-\tilde{s})^4\frac{\partial^2 U}{\partial s^2} + \frac{1}{4}(2-\tilde{t})^4\frac{\partial^2 U}{\partial t^2} - E(\tilde{s})\frac{\partial U}{\partial \tilde{s}} + F(\tilde{t})\frac{\partial U}{\partial \tilde{t}}\Big] = \lambda U, \tag{15}$$

$$D(\tilde{s},\tilde{t})\Big\{P\frac{\partial U}{\partial \tilde{t}} + 4P^2 N + 2P\Big[N + (1-\tilde{s})^2\frac{\partial N}{\partial \tilde{s}}\Big]\Big\} = -\lambda N, \tag{16}$$

where

$$\begin{aligned} C(\tilde{s},\tilde{t}) &= \Big[(\frac{\tilde{s}}{1-\tilde{s}})^2 + (\frac{\tilde{t}}{2-\tilde{t}})^2\Big]^{-1}, \quad D(\tilde{s},\tilde{t}) = \Big[1 + (\frac{\tilde{s}}{1-\tilde{s}})^2\Big]^{-1}, \\ E(\tilde{s}) &= 2(1-\tilde{s})^3 + 2P\tilde{s}(1-\tilde{s}), \text{ and } F(\tilde{t}) = -\frac{1}{2}(2-\tilde{t})^3 + P\tilde{t}(2-\tilde{t}). \end{aligned}$$

Let $\tilde{s}_i = i\Delta\tilde{s}$, $\tilde{t}_j = j\Delta\tilde{t}$, $U_{ij} = U(\tilde{s}_i,\tilde{t}_j)$, and $N_i = N(\tilde{s}_i)$. The standard centered difference formula is used to discretize the equation (15). We replace $\partial^2 U/\partial\tilde{s}^2$, $\partial^2 U/\partial\tilde{t}^2$, $\partial U/\partial\tilde{s}$ and $\partial U/\partial\tilde{t}$ with

$$\frac{U_{i+1,j} - 2U_{i,j} + U_{i-1,j}}{(\Delta\tilde{s})^2}, \qquad \frac{U_{i,j+1} - 2U_{i,j} + U_{i,j-1}}{(\Delta\tilde{t})^2},$$
$$\frac{U_{i,j+1} - U_{i,j-1}}{2\Delta\tilde{s}}, \qquad \frac{U_{i+1,j} - U_{i-1,j}}{2\Delta\tilde{t}}$$

respectively. At the boundary $\tilde{s} = 0$ and $\tilde{s} = 1$, we use ghost values $U_{-1,j} = U_{1,j}$, $U_{n+1,j} = U_{n-1,j}$ and centered difference to discretize $\partial U/\partial\tilde{s}$. *i.e.,*

$$\partial U/\partial\tilde{s} \approx \frac{U_{1,j} - U_{-1,j}}{2\Delta\tilde{s}}, \text{ at } \tilde{s} = 0 \tag{17}$$

$$\partial U/\partial\tilde{s} \approx \frac{U_{n-1,j} - U_{n+1,j}}{2\Delta\tilde{s}}, \text{ at } \tilde{s} = 1. \tag{18}$$

A similar scheme is used to discretize $\partial U/\partial\tilde{t}$ at $\tilde{t} = 2$. At the interface boundary $\tilde{t} = 1$, the temperature $U_{i,0}$ and the displacement of the moving front N_i satisfies $U_{i,0} = 2PN_i$. To avoid mixing U and N values, an upwind difference scheme

$$\partial U/\partial\tilde{t} \approx \frac{1}{\Delta\tilde{t}}\Big(-\frac{3}{2}U_{i,0} + 2U_{i,1} - \frac{U_{i,2}}{2}\Big).$$

is used to discretize the term $\partial U/\partial\tilde{t}$ in (16). The term $\partial N/\partial\tilde{s}$ is approximated by centered difference.

The above discretization scheme gives rise to an algebraic eigenvalue problem

$$Ax = \lambda x, \quad \text{where}$$

$$x = \begin{bmatrix} U_1 \\ \vdots \\ U_m \\ N \end{bmatrix}, \quad U_j = \begin{bmatrix} U_{0,j} \\ \vdots \\ U_{n,j} \end{bmatrix} \quad \text{and} \quad N = \begin{bmatrix} N_0 \\ \vdots \\ N_n \end{bmatrix}$$

The structure of a typical A is demonstrated in Figure 1. Eigenvalues of positive real

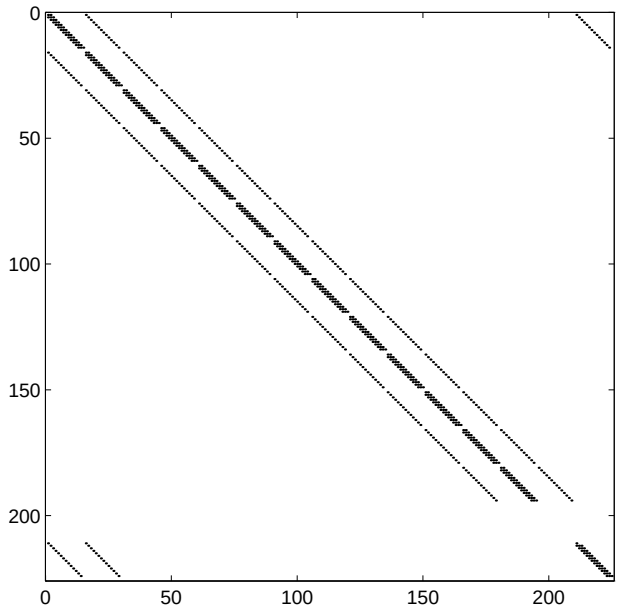

FIG. 1. *The structure of the coefficent matrix.*

parts are sought to determine interesting unstable modes that involve excitation of the interface. Analysis [5] suggests that at least part of the spectrum corresponding to this eigenvalue problem is continuous and unbounded. The conventional QR method become expensive as the mesh size of the discretization gets small. Fast iterative scheme such as the Arnoldi method is attractive in this setting.

5. Implicitly Restarted Arnoldi Method. The standard Arnoldi method computes a factorization of the form

$$AV_k = V_k H_k + f e_k^T, \quad V_k^H V_k = I, \quad \text{and} \quad V_k^H f = 0,$$

where H_k is a $k \times k$ upper Hessenberg matrix. The first column of V_k is arbitrarily chosen and normalized such that $\|v_1\| = 1$. Subsequent columns of V_k, the matrix H_k and the vector f are generated from the Arnoldi process illustrated below.

Input: $(A,\ v_1)$
Output: $(V_k,\ H_k,\ f)$
$w \leftarrow Av$; $\alpha_1 = v_1^H w$;
$H_1 = (\alpha_1)$; $V_1 = (v_1)$; $f \leftarrow w - v_1\alpha_1$;
for $j = 1, 2, 3, ..., k-1$

1. $\beta_j = \|f\|$; $v_{j+1} \leftarrow f/\beta_j$
2. $V_{j+1} = (V_j,\ v_{j+1})$; $H_j \leftarrow \begin{pmatrix} H_j \\ \beta_j e_j^T \end{pmatrix}$;
3. $z \leftarrow Av_{j+1}$;
4. $h \leftarrow V_j^H z$; $H_{j+1} = (H_j,\ h)$;
5. $f \leftarrow z - V_{j+1}h$;

end;

It can be verified that the columns of V_k form an orthonormal basis for the Krylov subspace $\mathcal{K} = \{v_1, Av_1, ..., A^{k-1}v_1\}$. Eigenvalues of H_k provide approximations to the eigenvalues of A. They are often referred to as the Ritz values. If y is the eigenvector of H_k corresponding to an eigenvalue θ, the Ritz vector $z = V_k y$ is an approximation to an eigenvector of A. It is well known that Ritz values converges rapidly to well separated extreme eigenvalues. However, in our problem these eigenvalues correspond to the ones on the left half of the real axis, and are not interesting. (The full spectrum of the A derived from a coarse discretization is shown in Figure 2.) To overcome this difficulty,

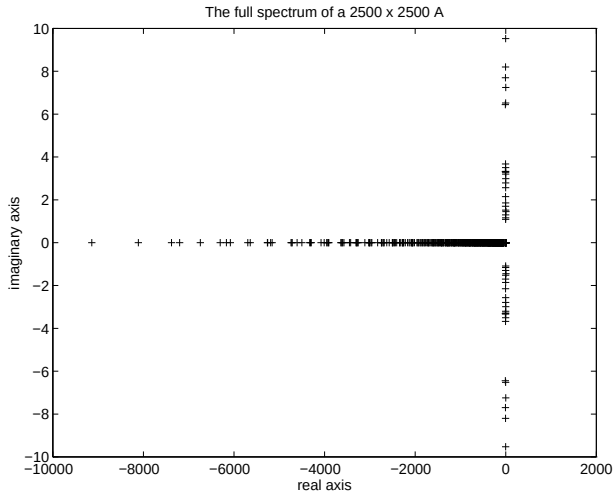

FIG. 2. *The full spectrum of a* 2500×2500 A .

one must construct a starting vector v_1 such that the subspace spanned by columns of V_k contains the desired eigencomponents. The construction of v_1 is not trivial. The Implicitly Restarted Arnoldi Method (IRAM) [7] provides an efficient scheme to repeatedly modify an arbitrary starting vector v_1 so that the unwanted eigencomponents v_1 are annihilated by a polynomial in A. The analysis and some of the implementation issues of IRAM are also contained in [4]. The basic theory is outlined below.

Given a $(k+p)$-step Arnoldi factorization

$$AV_{k+p} = V_{k+p}H_{k+p} + fe_{k+p}^T, \quad V_{k+p}^H V_{k+p} = I, \quad V_{k+p}^H f = 0, \tag{19}$$

a sequence of QR updates corresponding to the shifts $\mu_1, \mu_2, ..., \mu_p$ may be applied as follows. Let $H_{k+p} - \mu_1 I = Q_1 R_1$ be the QR decomposition of $H_{k+p} - \mu_1 I$, it follows from (19) that

$$(A - \mu_1 I)V_{k+p} = V_{k+p}(H_{k+p} - \mu_1 I) + fe_{k+p}^T = (V_{k+p}Q_1)R_1 + fe_{k+p}^T. \tag{20}$$

Multiplying the above equation on the right by Q_1 yields

$$(A - \mu_1 I)(V_{k+p}Q_1) = (V_{k+p}Q_1)(Q_1^H H_{k+p}Q_1) + fe_{k+p}^T Q_1.$$

It is easily seen from (20) that the first column of the updated $V_{k+p}^+ = V_{k+p}Q_1$ is related to the first column of V_{k+p} through $(A - \mu_1 I)v_1 = v_1^+ \rho_{11}$. Let $H_{k+p}^+ = Q_{j-1}^H H Q_{j-1}$. The next cycle of IRAM starts with the factorization of $H_{k+p}^+ - \mu_2 I$ followed by the update of V_{k+p}^+ and H_{k+p}^+. After all p shifts have been used, the Arnoldi factorization can be recovered by dropping the last p columns of V_{k+p}^+ and H_{k+p}^+ and performing p more steps of Arnoldi iteration to give

$$AV_{k+p}^+ = V_{k+p}^+ H_{k+p}^+ + f^+ e_{k+p}^T.$$

This is equivalent to a new Arnoldi factorization with v_1 replaced by $v_1^+ = P_p(A)v_1$, where $P_p(\lambda)$ is a polynomial with roots at $\mu_1, \mu_2, ..., \mu_p$. This polynomial is designed to filter out the unwanted eigen-components in the original starting vector v_1. Thus the shifts $\mu_1, \mu_2, ..., \mu_p$ are chosen to be approximations to the unwanted eigenvalues of A. The above process is repeated until all k desired eigenvalues of A are extracted from H_{k+p}^+. Error estimates and deflation techniques for IRAM are explained in detail in [4].

A software package based on this algorithm, ARPACK is used successfully in our computation. Table 1 lists the leading eigenvalues that corresponds to different levels discretization and the number of matrix vector multiplications (MATVECs) and CPU time used to obtain them. The *Peclet* number is set to be 0.1 in our computation. The experiment is performed on a SUN-SPARC 10. For coarse discretization up to about $\Delta\tilde{s} = \Delta\tilde{t} = 1/29$, the results compared favorably to those obtained from the LAPACK [1]. As the matrix size increases, the computation becomes more expensive as indicated by a large number of matrix vector multiplications used. In the case $\Delta\tilde{s} = \Delta\tilde{t} = 1/99$, IRAM did not converge in 300 iterations.

An alternative to compute the eigenvalues of A directly is to work with $(A - \sigma I)^{-1}$, where σ is an estimated location of desired eigenvalue. Since eigenvalues of $(A - \sigma I)^{-1}$ are often large and well separated, the Arnoldi approximation converges extremely fast. However, the fast convergence is obtained at the cost of factoring the matrix $(A - \sigma I)$ and solving a linear system $(A - \sigma I)w = v$ at each iteration. In our application, the matrix can be easily factored using a block Guass elimination. The initial shift can be predicted from the runs of smaller size problems. In Table 2 we list the number of linear system solved (LSs) and the CPU time used for problems of various size. It is observed that using ARPACK in shift-invert mode is considerably faster in this application.

matrix size	eigenvalue	MATVECs	CPU(seconds)
2500	6.39	4381	876.68
3600	7.78	6645	1252.61
4900	9.17	10406	2664.33
6400	10.6	10508	3847.50

TABLE 1

The performance of ARPACK in direct mode. Three eigenvalues are found in each run. Parameters k and p are set to be 4 and 40 repectively.

matrix size	LSs	CPU(seconds)
2500	121	44.09
3600	121	69.19
4900	87	73.88
6400	88	107.25
8100	86	147.88
10000	83	188.95

TABLE 2

The performance of ARPACK in shift-invert mode. The shift used is $\sigma = 15.0$. Ten eigenvalues are found in each run. Parameters k and p are set to be 10 and 50 respectively.

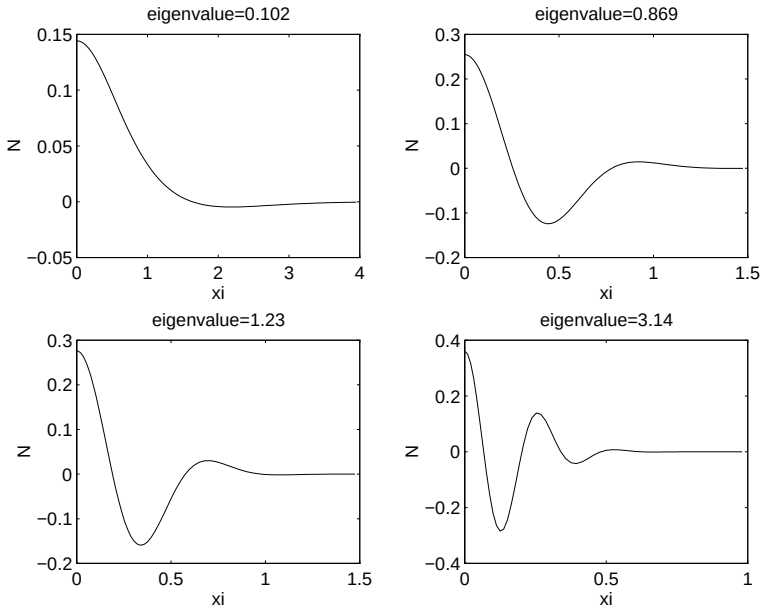

FIG. 3. *The interface N associated with different eigenvalues*

6. Numerical Results. Our computation shows that there are many eigenvalues of A with positive real parts. This implies that the solidification of the needle crystal is unstable. It is also observed in our computation that the leading eigenvalue increases as $\Delta\tilde{s}$ and $\Delta\tilde{t}$ decrease. This agrees with the analytic prediction that eigenvalues are unbounded as $\Delta\tilde{s}, \Delta\tilde{t} \to 0$. The computed interface N for the disturbance equation corresponding to the four positive eigenvalues of A are plotted in Figure 3. The computation is done on a grid with $\Delta\tilde{s} = \Delta\tilde{t} = 1/99$. It is observed that as the eigenvalue increases, the interface becomes more oscillatory. This agrees with the result obtained from analysis [5]. Finally the temperature field U in both phases that corresponds to a typical positive eigenvalue is plotted in Figure 4. The contour plots of the temperature fields corresponding to the four interfaces shown in Figure 3 are demonstrated in Figure 5.

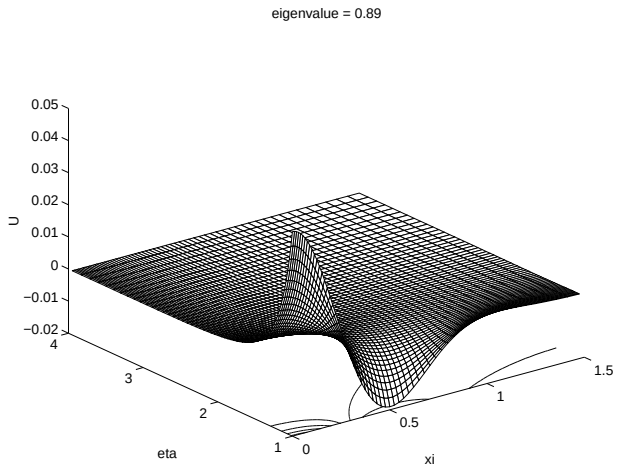

FIG. 4. *The temperature field associated with* $\lambda = 0.869$.

REFERENCES

[1] E. Anderson, Z. Bai, C. Bischof, J. Demmel, J. Dongarra, J. Du Croz, A. Greenbaum, S. Hammarling, A. McKenney, S. Ostrouchov, and D. Sorensen. *LAPACK Users' Guide*. SIAM, Philadelphia, PA., second edition, 1992.

[2] K. Brattkus and D. I. Meiron. Numerical simulations of unsteady crystal growth. *SIAM Journal on Applied Mathematics*, 52(5):1303–1320, October 1992.

[3] G. P. Ivantsov. Mathematical physics. *Dokl. Akad. Nauk. SSSR*, 58:567, 1947. Translaftted by G. Horvay. Report No. 60-RL-(2511M), G.E. research Lab., Schenectedy, New York, 1960.

[4] R. B. Lehoucq. *Analysis and Implementation of an Implicitly Restarted Arnoldi Iteration*. PhD thesis, Department of Computational and Applied Mathematics, Rice University, Houston, TX, 1995.

[5] D. I. Meiron. Private communication, 1996.

[6] J. A. Sethian and J. Strain. Crystal growth and dendritic solidification. *Journal of Computational Physics*, 98:231–253, 1992.

[7] D. C. Sorensen. Implicit application of polynomial filters in a k-step Arnoldi method. *SIAM Journal on Matrix Analysis and Applications*, 13(1):357–385, January 1992.

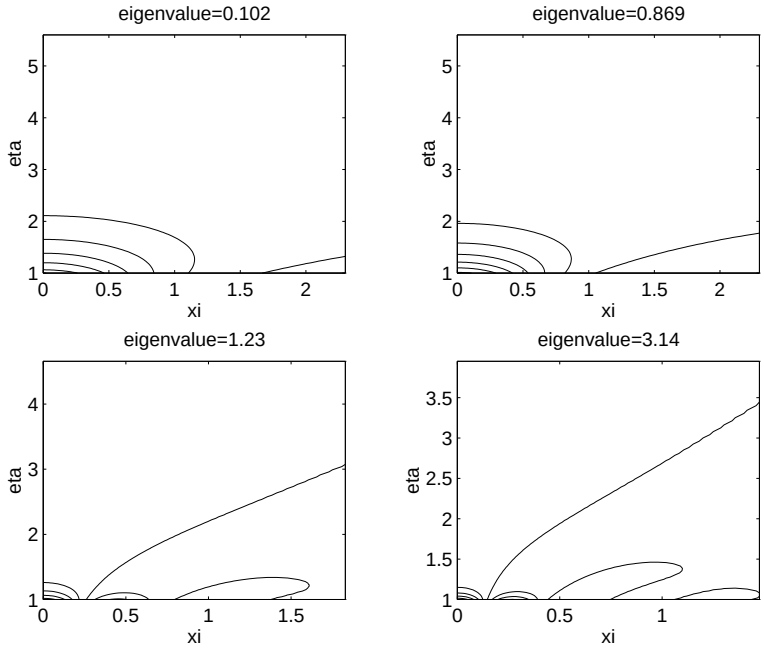

FIG. 5. *The temperature associated with various eigenvalues.*